

1  
2  
3  
4  
5  
6  
7  
8  
9  
10  
11  
12  
13  
14  
15  
16  
17  
18  
19  
20  
21

## **SARS-CoV-2 Delta Spike Protein Enhances the Viral Fusogenicity and Inflammatory Cytokine Production**

Zhujun Ao <sup>#</sup>, Maggie Jing Ouyang <sup>#</sup>, Titus Abiola Olukitibi, and Xiaojian Yao<sup>\*</sup>

Laboratory of Molecular Human Retrovirology, Department of Medical Microbiology, Max Rady College of Medicine, Rady Faculty of Health Sciences, University of Manitoba, Winnipeg, MB, Canada.

<sup>#</sup>. Both authors contributed equally to this work

<sup>\*</sup> To whom correspondence should be addressed:

X-j. Yao, Laboratory of Molecular Human Retrovirology, Department of Medical Microbiology, Max Rady College of Medicine, Rady Faculty of Health Sciences, University of Manitoba ([xiaojian.yao@umanitoba.ca](mailto:xiaojian.yao@umanitoba.ca))

22

23 **SUMMARY**

24 The Delta variant is now the most dominant and virulent SARS-CoV-2 variant of concern  
25 (VOC). In this study, we investigated several virological features of Delta spike protein (SP<sub>Delta</sub>),  
26 including protein maturation and its impact on viral entry of cell-free pseudotyped virus, cell-cell  
27 fusion ability and its induction of inflammatory cytokine production in human macrophages and  
28 dendritic cells. The results showed that SPΔC<sub>Delta</sub> exhibited enhanced S1/S2 cleavage in cells and  
29 pseudotyped virus-like particles (PVLPs). We further showed that SPΔC<sub>Delta</sub> elevated  
30 pseudovirus infection in human lung cell lines and mediated significantly enhanced syncytia  
31 formation. Furthermore, we revealed that SPΔC<sub>Delta</sub>-PVLPs had stronger effects on stimulating  
32 NF-κB and AP-1 signaling in human monocytic THP1 cells and induced significantly higher  
33 levels of pro-inflammatory cytokine, such as TNF-α, IL-1β and IL-6, released from human  
34 macrophages and dendritic cells. Overall, these studies provide evidence to support the important  
35 role of SPΔC<sub>Delta</sub> during virus infection, transmission and pathogenesis.

36

37 **Keywords:** COVID-19, SARS-CoV-2, Delta variant, Spike protein, cell-to-cell fusion, NF-κB  
38 pathway, proinflammatory cytokines

39

40

## 41 INTRODUCTION

42 The emergence of the highly pathogenic coronavirus disease 2019 (COVID-19) has been a major  
43 concern and threat to public health for two years. As of early November 2021, approximately  
44 248 million COVID-19 cases and more than 5 million deaths were reported globally (WHO,  
45 2021). COVID-19 is caused by severe acute respiratory syndrome coronavirus 2 (SARS-CoV-2),  
46 which is a member of betacoronaviridae with a single-stranded 30 kb positive-sense RNA  
47 genome encoding 29 proteins (Srivastava et al., 2021). Within 2 years, multiple variants of  
48 SARS-CoV-2 have emerged (Galloway et al., 2021; Greaney et al., 2021; Nonaka et al., 2021;  
49 Paiva et al., 2021; Resende et al., 2021; Santos and Passos, 2021; Tegally et al., 2020; Volz et  
50 al., 2021). Delta variant, which was first detected in India and derived from the Pango lineage  
51 B.1.617.2, is the most dominant variant of concern (VOC) and has accounted for approximately  
52 99% of new cases of coronavirus worldwide (Banu et al., 2020; Ranjan et al., 2021; Sahoo et al.,  
53 2021; Worldometer, 2021). Previous studies suggested that Delta variant infection has a shorter  
54 incubation period but a greater viral load ( $> 1,000$  times) than earlier variants (Li et al., 2021;  
55 Reardon, 2021). Further, the patients contracted with Delta variant have higher hospitalization  
56 rate and more severe outcomes (Twohig et al., 2021). Unfortunately, current vaccines only  
57 provide partial protection against the infection of Delta variant, because these vaccines are  
58 designed based on the original Wuhan-Hu-1 sequence (Mlcochova et al., 2021). Therefore, it is  
59 important to understand the molecular mechanisms of the increased transmissibility and immune  
60 evasion of these SARS-CoV-2 variants to facilitate the development of vaccines and therapeutic  
61 drugs against COVID-19.

62 VOCs are mainly classified based on the mutations on their spike protein (SP). The SP of  
63 coronavirus is responsible for viral attachment and entry to the host cells (Huang et al., 2020b).

64 The matured SP is cleaved to generate S1 and S2 subunits at specific cleavage sites. The S1  
65 subunit (aa 14-685) is responsible for receptor binding through its receptor-binding domain  
66 (RBD). The S2 subunit (aa 686-1273) mediates membrane fusion to facilitate cell entry (Bertram  
67 et al., 2013; Hoffmann et al., 2020b; Peacock et al., 2021b). Mutations in SP have resulted in the  
68 high rates of transmission and replication of various variants (Zhang et al., 2021a; Zhou et al.,  
69 2021) and the immune evasion from antibody neutralization of various variants (McCallum et  
70 al.; Mlcochova et al., 2021; Zhang et al.). The SP of the Delta variant has eight mutations  
71 compared with the original virus, including T19R,  $\Delta$ 156– $\Delta$ 157, and R158G in the N-terminus  
72 Domain (NTD), D614G, L452R and T478K at the RBD, P681R close to the furin cleavage site,  
73 and D950N at the S2 region (Cherian et al., 2021; Planas et al., 2021; Zhang et al., 2021a). It has  
74 been demonstrated that the mutations at the NTD of Delta SP alter the antigenic surface near the  
75 NTD-1 epitope, thus leading to the lack of binding affinity with the NTD neutralizing antibodies  
76 (Zhang et al., 2021a).

77 Furthermore, the P681R mutation closed to the furin cleavage has been demonstrated to  
78 aid the pathogenicity of the virus (Cherian et al., 2021; Liu et al., 2021; Saito et al., 2021). The  
79 newly identified furin cleavage site (681-PRRAR↓SV-687) at the S1/S2 site is reported to be  
80 critical for the pathogenesis of SARS-CoV-2 in mouse models, and also be responsible for the  
81 cell-cell fusion, which is absent in other group-2B coronaviruses (Coutard et al., 2020; Johnson  
82 et al., 2020; Xia et al., 2020). It was shown that P681R mutation at this cleavage site endow  
83 Delta variant with special features that facilitate the spike protein cleavage and viral fusogenicity  
84 (Peacock et al., 2021b; Saito et al., 2021). Study found that a chimeric Delta SARS-CoV-2  
85 bearing the Alpha-SP replicated less efficiently than the wild-type Delta variant, and the  
86 reversion of Delta P681R mutation to wild-type P681 attenuated Delta variant replication as well

87 (Liu et al., 2021). These observations suggested that the P618R mutation that occurs in Delta  
88 variants contributes immensely to the high replication and transmissibility rate. We are therefore  
89 interested in further investigating how the P618R mutation impacts the high replication rate of  
90 Delta variants.

91 Like other high pathogenic viruses (influenza H5N1, SARS-CoV-1 and MERS-CoV),  
92 SARS-CoV-2 infection also induced excessive inflammatory response with the release of a large  
93 amount of pro-inflammatory cytokines (cytokine storm) that may result in Acute Respiratory  
94 Distress Syndrome (ARDS) and multiorgan damage (Zhu and al., 2020). Clinical studies showed  
95 that the high mortality of COVID-19 is related to cytokine release syndrome (CRS) in a  
96 subgroup of severe patients (Huang et al., 2020a), characterized by elevated levels of certain  
97 cytokines including IL-6, TNF- $\alpha$ , IL-8, IL-1 $\beta$ , IL-10, MCP-1 and IP-10 (Hadjadj et al., 2020;  
98 Huang et al., 2020a; Mehta et al., 2020; Xu et al., 2020; Yang et al., 2020). The observed  
99 cytokine production induced by SARS-CoV-2 infection or spike protein expression has been  
100 linked with nuclear factor kappa B (NF- $\kappa$ B) and and activator protein-1(AP-1) signaling  
101 pathways that can induce the expression of a variety of proinflammatory cytokine genes  
102 (Neufeldt et al., 2020b; Zhu et al., 2021). Like other RNA virus, SARS-CoV-2 was found  
103 activate NF- $\kappa$ B and AP-1 transcription factors following the sensing of viral RNAs or proteins  
104 by different pathogen pattern recognition receptors (PRRs) and associated signalling cascades,  
105 including RLRs and TLRs (Pantazi et al., 2021; Zhu et al., 2021). In addition, angiotensin II type  
106 1 receptor (AT1)-MAPK signalling (Patra et al., 2020) and the cGAS-STING signalling  
107 (Neufeldt et al., 2020a) have been identified responsible for the activation of NF- $\kappa$ B and the  
108 elevated expression of IL-6 in the SARS-CoV-2 infected or SP expressing cells. However,

109 whether Delta variant or its SP may initiate stronger cytokine storm in patients that leading to  
110 more severe illness than other strains still required more investigation.

111 The current study aims to characterize the cleavage/maturation of various SPs of SARS-  
112 CoV-2, especially the Delta variant SP, and their effects on virus infection, cell-cell fusion,  
113 cytokine production and related signaling pathways. By using a SARS-CoV-2 SP pseudotyped  
114 lentiviral vector or viral-like particles (PVLPs), we demonstrated that SP<sub>Delta</sub> enhanced S1/S2  
115 cleavage, accelerated pseudovirus infection and promoted cell-cell fusion. We also showed that  
116 SP<sub>Delta</sub> strongly activates NF- $\kappa$ B and AP-1 signaling in THP1 cells. Furthermore, we observed  
117 that SP $\Delta$ C<sub>Delta</sub>-PVLV stimulation promoted the production of several pro-inflammatory cytokines  
118 by human macrophages and dendritic cells.

119

## 120 **RESULTS**

### 121 **SARS-CoV-2 Delta SP exhibited enhanced cleavage and maturation in cells and in the** 122 **pseudotyped virus**

123 To investigate the functional role of SARS-CoV-2 Delta SP, we first synthesized cDNA  
124 encoding SARS-CoV-2 Delta SP, as described in CDC's SARS-CoV-2 Variant Classifications  
125 and Definitions (CDC, 2021) (Fig. 1A) and inserted cDNA into a pCAGG-expressing plasmid,  
126 as described in the Materials and Methods. Previously described pCAGG-SP $\Delta$ C<sub>WT</sub>- and pCAGG-  
127 SP $\Delta$ C<sub>G614</sub>-expressing plasmids (Ao et al., 2021a) were also used in this study. Meanwhile, we  
128 constructed a pCAGG-SP $\Delta$ C<sub>Delta</sub>-PD in which arginine (R) at the amino acid position of 681 and  
129 asparagine (N) at 950 in SP $\Delta$ C<sub>Delta</sub> were reverted to the original proline (P) and aspartic acid (D)  
130 to test the effect of these amino acids on the function of SP $\Delta$ C<sub>Delta</sub> (Fig. 1A). To enhance the

131 transportation of SP to the cell surface and increase the virus incorporation of SP, the cDNA  
132 encoding the C-terminal 17 aa in SARS-CoV-2 SP was deleted in all pCAGG-SP $\Delta$ C plasmids  
133 (Ao et al., 2021a).

134 To examine the expression of various SPs in the cells and their incorporation in the SP $\Delta$ C-  
135 pseudotyped viral particles (PVPs), each SP $\Delta$ C-expressing plasmid was cotransfected with a  
136 multiple-gene deleted HIV-based vector encoding a Gaussia luciferase gene ( $\Delta$ RI/ $\Delta$ Env/Gluc)  
137 and a packaging plasmid (pCMV $\Delta$ R8.2) in HEK293T cells, as described previously (Ao et al.,  
138 2021a). After 48 hrs of transfection, the expression of each SP $\Delta$ C in the transfected cells was  
139 analyzed by an indirect immunofluorescence (IF) assay using human SARS-CoV-2 S-NTD  
140 antibodies. The results revealed that all SP $\Delta$ Cs were well expressed in the transfected cells or  
141 cell surface (Fig. 1B). Meanwhile, the transfected cells and PVPs were lysed and processed with  
142 WB with anti-SP/RBD or anti-S2 antibodies, respectively (Fig. 1C, top and middle panels).  
143 Interestingly, the data clearly showed that in the cells, SP $\Delta$ C<sub>Delta</sub> was more efficiently processed  
144 from the S precursor into S1 and S2 than SP $\Delta$ C<sub>WT</sub> and SP $\Delta$ C<sub>G614</sub> (Fig. 1C, compare Lane 3 to  
145 Lanes 1 and 2). In PVPs, the majority of SP $\Delta$ C<sub>Delta</sub> presented as a mature form (S1 and S2)  
146 compared to SP $\Delta$ C<sub>WT</sub> and SP $\Delta$ C<sub>G614</sub> (Fig. 1C, compare Lane 7 to Lanes 5 and 6), indicating that  
147 SP $\Delta$ C<sub>Delta</sub> undergoes a more efficient maturation process. Surprisingly, S1 of SP $\Delta$ C<sub>Delta</sub> but not  
148 S2 appeared to migrate faster than S1 of SP $\Delta$ C<sub>WT</sub> and SP $\Delta$ C<sub>G614</sub> (Fig. 1C, top panel). The  
149 possible mechanism for this behavior is currently unknown.

150 The cleavage of the SARS-CoV-2 SP into S1 and S2 most likely occurs by furin, and the  
151 P681R mutation of the SP Delta was suggested to enhance S1/S2 cleavability (Liu et al., 2021;  
152 Peacock et al., 2021a). We therefore further tested whether a fusin protease inhibitor, a peptidyl

153 chloromethylketone (CMK), or the reverse change in R<sub>681</sub> of SPAC<sub>Delta</sub> to P would alter the  
154 maturation rate of the S protein. The SPAC<sub>Delta-PD</sub>-PVPs or SPAC<sub>Delta</sub>-PVPs packaged in the  
155 presence or absence of CMK were analyzed by WB with anti-RBD antibody and quantified by  
156 densitometry using ImageJ (<https://imagej.nih.gov/ij/>). The results showed that either CMK  
157 treatment or SPAC<sub>Delta-PD</sub> clearly negatively impacted the maturation of SPAC<sub>Delta</sub> (Fig. 1D).

158

### 159 **Delta-SP mediates more efficient pseudovirus infection in a lung epithelial cell line and** 160 **primary macrophages**

161 To investigate the impact of SPAC<sub>Delta</sub> on viral infection, we produced Gluc-expressing Delta-  
162 SP-PVPs (Fig. 2A) and tested the infectivity of different pseudoviruses in two human lung  
163 epithelial cell lines, Calu-3 and A549 cells. To increase susceptibility to SP-PVP infection, the  
164 A549<sub>ACE2</sub> cell line was generated by transducing a lentivirus expressing hACE2 and subsequent  
165 puromycin selection, as described in the Materials and Methods. hACE2 expression in A549<sub>ACE2</sub>  
166 cells was verified by WB (Fig. 2B). Then, both cell lines were infected with equivalent amounts  
167 (adjusted with p24 values) of the SPAC<sub>WT</sub>-, SPAC<sub>G614</sub>-, and SPAC<sub>Delta</sub>-PVPs for three hours and  
168 washed. At 24 and 48 hrs post infection (p.i.), the supernatants were collected, and the infection  
169 levels of pseudoviruses were monitored by measuring Gluc activity. The results showed that in  
170 both cell lines, the SPAC<sub>Delta</sub>-PVPs exhibited the highest infection efficiency, the SPAC<sub>G614</sub>-  
171 PVPs had a slightly lower infection efficiency than SPAC<sub>Delta</sub>, while the SPAC<sub>WT</sub>-PVPs showed a  
172 significantly lower infection efficiency (Fig. 2C). All of these results indicated that SPAC<sub>Delta</sub>-  
173 PVPs had a significantly more efficient virus entry step than SPAC<sub>WT</sub>-PVPs in a single cycle  
174 replication system.



175 Next, we also checked the ability of SP $\Delta$ C-PVPs to infect human differentiated  
176 macrophages and dendritic cells. Briefly, human monocyte-derived macrophages (MDMs) or  
177 dendritic cells (MDDCs) were infected with equal amounts (adjusted with HIV p24 levels) of  
178 SP $\Delta$ C<sub>wt-</sub>, SP $\Delta$ C<sub>G614-</sub>, and SP $\Delta$ C<sub>Delta-</sub>-PVPs. At 48 and 72 hrs p.i., the Gluc activity in the  
179 supernatant from the infected cell cultures was monitored. The results showed that both human  
180 primary cells, especially MDMs, could be infected by SP $\Delta$ C-PVPs, while SP $\Delta$ C<sub>Delta-</sub> and  
181 SP $\Delta$ C<sub>G614-</sub>-PVPs displayed more efficient infection than SP $\Delta$ C<sub>wt-</sub>-PVPs (Fig. 2D). All of these  
182 experimental observations indicate that SP $\Delta$ C<sub>Delta-</sub>-PVPs have a stronger ability to target MDMs  
183 than SP $\Delta$ C<sub>wt-</sub>-PVPs. The results also suggested that MDDCs can be targeted by SP $\Delta$ C-PVPs but  
184 with less efficiency.

185

## 186 **Delta-SP variant enhanced syncytia formation in lung epithelial A549 cells expressing** 187 **ACE2**

188 Previous studies have shown that SARS-CoV-2 SP is able to possess fusogenic activity and form  
189 large multinucleated cells (syncytia formation) (Bussania et al., 2020; Cattin-Ortola' et al., 2020).  
190 We then asked whether Delta-SP could possess higher fusogenic activity than other variants.  
191 Briefly, 293T cells were transfected with SP $\Delta$ C<sub>WT</sub>, SP $\Delta$ C<sub>G614</sub>, SP $\Delta$ C<sub>Delta</sub>, or SP $\Delta$ C<sub>DeltaPD</sub> plasmids  
192 by Lipofectamine 2000. At 24 hrs of transfection, we mixed SP $\Delta$ C-expressing 293T cells with  
193 A549<sub>ACE2</sub> cells at a ratio of 1:3. At 6 and 30 hrs post transfection, syncytial formation was  
194 observed under a microscope, and the results revealed that SP $\Delta$ C<sub>WT</sub> and SP $\Delta$ C<sub>G614</sub> induced  
195 similar levels and sizes of syncytia. Intriguingly, an increasing number of syncytia formations  
196 were observed in the coculture of SP $\Delta$ C<sub>Delta</sub>-expressing 293T and A549<sub>ACE2</sub> cells (Fig. 3A and  
197 B), indicating that SP from the Delta variant has a stronger fusogenic ability. However,

198 SPAC<sub>DeltaPD</sub>-expressing 293T/A549<sub>ACE2</sub> cell coculture displayed less syncytia formation than  
199 SPAC<sub>Delta</sub> (Fig. 3 B). A and B), suggesting the importance of P681R for the strong fusogenic  
200 activity of SP from the Delta variant.

201 To further confirm the strong fusogenic ability of SPAC<sub>Delta</sub>, we also generated A549  
202 cells stably expressing SPAC<sub>wt</sub>, SPAC<sub>G614</sub> or SPAC<sub>Delta</sub> (named A549-SPAC<sub>Delta</sub>, A549-SPAC<sub>G614</sub>  
203 or A549-SPAC<sub>wt</sub> cells) (Fig. 3C). Since A549-SPAC<sub>wt</sub> and A549-SPAC<sub>Delta</sub> cells displayed  
204 similar levels of SPAC expression based on a WB analysis, we then tested their fusogenic ability  
205 by mixing A549-SPAC<sub>Delta</sub> or A549-SPAC<sub>wt</sub> cells with the A549<sub>ACE2</sub> cell line using a similar  
206 experimental process as described above. Meanwhile, A549-SPAC<sub>Delta</sub> or A549-SPAC<sub>wt</sub> cells  
207 were cocultured with A549 cells as a control. The results confirmed that the coculture of A549-  
208 SPAC<sub>Delta</sub> cells and A549<sub>ACE2</sub> cells formed large syncytia formation more efficiently than that of  
209 A549-SPAC<sub>wt</sub> cells (Fig. 3D), confirming the stronger fusogenic activity of the SP of the Delta  
210 variant.

211

### 212 **Delta variant SP stimulates higher NFκB and AP1 signaling pathway activities**

213 The severity of COVID-19 is highly correlated with dysregulated and excessive release of  
214 proinflammatory cytokines (Huang et al., 2020a). Given that the NFκB and AP1 signaling  
215 pathways are among the critical pathways responsible for the expression of proinflammatory  
216 cytokines and chemokines (Hojyo et al., 2020; Kawasaki and Kawai, 2014), we therefore  
217 examined the activities of these two signaling pathways triggered by SPAC in the monocyte cell  
218 line THP1 and THP1-derived macrophages. First, we generated THP1-NF-κB-Luc and THP1-  
219 AP-1-Luc sensor cell lines by transducing THP1 cells with a lentiviral vector encoding the  
220 luciferase reporter gene driven by NFκB- or AP1-activated transcription response elements (Fig.

221 4A), as described in the Materials and Methods. To obtain THP1-derived macrophages, THP1-  
222 NF- $\kappa$ B-Luc and THP1-AP-1-Luc sensor cell lines were treated with phorbol 12-myristate 13-  
223 acetate (PMA) (100 nM) for 3 days. Additionally, we produced genome-free SP $\Delta$ C-PVLPs by  
224 cotransfecting each SP $\Delta$ C-expressing plasmid with a packaging plasmid (pCMV $\Delta$ R8.2) in 293T  
225 cells, and the expression of SP $\Delta$ C in the purified PVLPs was verified by WB with an anti-RBD  
226 antibody (Fig. 4B). Then, different THP1 sensor cell lines and THP1-derived macrophages were  
227 treated with different SP $\Delta$ C-PVLPs of same amount (adjusted by p24) for 6 hrs, and the  
228 luciferase activity in treated cells was measured by a luciferase assay system (Promega).  
229 Interestingly, we found that the NF $\kappa$ B activity induced by SP $\Delta$ C<sub>wt</sub> and SP $\Delta$ C<sub>G614</sub>-PVLPs was  
230 slightly higher than that induced by the VLP control (Gag). However, the SP $\Delta$ C<sub>Delta</sub>-treated  
231 THP1 cells/macrophages produced significantly higher (3~7-fold) NF $\kappa$ B activity compared with  
232 SP $\Delta$ C<sub>wt</sub> or SP $\Delta$ C<sub>G614</sub> (Fig. 4C). Consistent with this finding, SP $\Delta$ C<sub>Delta</sub> also triggered higher (~2-  
233 fold) AP1 signaling pathway activities in THP1/macrophages than SP $\Delta$ C<sub>wt</sub> or SP $\Delta$ C<sub>G614</sub> (Fig.  
234 4D). These results indicated that SP $\Delta$ C<sub>Delta</sub> triggered significantly stronger signals to activate the  
235 NF $\kappa$ B and AP1 pathways in the monocyte cell line THP1 and THP1-derived macrophages.

236

### 237 **Delta variant SP stimulates higher proinflammatory cytokine production in human** 238 **macrophages (MDMs) and dendritic cells (MDDCs)**

239 Previous studies have shown that SARS-CoV-2 infection can stimulate the production of  
240 immunoregulatory cytokines (IL-6, IL-10) in human monocytes and macrophages (Boumaza et  
241 al., 2021). We further investigated whether SP of the Delta variant can induce higher levels of  
242 proinflammatory cytokine and chemokine in MDMs and MDDCs. Briefly, human MDMs and  
243 MDDCs were treated with the same amount (adjusted by p24) of SP $\Delta$ C-PVLPs, including

244 SPAC<sub>wt</sub><sup>-</sup>, SPAC<sub>G614</sub><sup>-</sup>, SPAC<sub>Delta</sub>-PVLPs or control VLPs (Gag-VLPs). After 24 hrs of incubation,  
245 the cytokines released in the supernatants were determined by a MSD (Meso Scale Discovery)  
246 immunoassay. The results revealed that SPAC<sub>wt</sub>-PVLP stimulation did not result in a significant  
247 change in cytokine release from MDMs compared to the control VLPs (Fig. 5A). However, in  
248 MDMs, SPAC<sub>Delta</sub>-PVLPs induced significantly higher levels of several proinflammatory  
249 cytokines, such as IFN- $\gamma$ , TNF- $\alpha$ , IL-1 $\beta$ , and IL-6, while SPAC<sub>G614</sub>-PVLPs also induced increase  
250 of these cytokines but overall to a less extent, when compared with SPAC<sub>wt</sub>-PVLPs (Fig. 5A).  
251 For example, the SPAC<sub>Delta</sub>-PVLPs elevated TNF- $\alpha$  level 61-fold in comparison with SPAC<sub>wt</sub>-  
252 PVLPs, contrastingly, SPAC<sub>G614</sub>-PVLPs only increased to approximately 33-fold. Nevertheless,  
253 all of SPAC-PVLPs showed no stimulating effects on IL-2 and IL-8 production. Interestingly,  
254 SPAC<sub>Delta</sub>-PVLPs and SPAC<sub>G614</sub>-PVLPs also slightly increased anti-inflammatory cytokines IL-  
255 4, IL-10 and IL-13, indicating the negative feedback of inflammation may exist during these  
256 stimulations.

257 Surprisingly, in MDDCs, SPAC<sub>Delta</sub>-PVLP stimulation resulted in a significant increase in  
258 most pro-inflammation cytokines we tested, including IFN- $\gamma$ , TNF- $\alpha$ , IL-1 $\beta$ , IL-2, IL-6, IL-8,  
259 and IL-12p70 (Fig. 5B). Among them, IL-6, TNF- $\alpha$  and IL-2 were the most increased cytokines  
260 (8~13-fold), followed by IFN- $\gamma$  and IL-1 $\beta$  (5~6-fold). The levels of IFN- $\gamma$ , IL-2, and IL-6 in the  
261 supernatans of SPAC<sub>G614</sub>-PVLPs treated MDDCs were higher than that of SPAC<sub>WT</sub>-PVLPs or  
262 control VLPs, also to a less extent. In contrast, IL-10 production appears to be negatively  
263 regulated by all SPAC-PVLPs, including the control VLPs. Altogether, the above results  
264 suggested that SPAC<sub>Delta</sub> could induce remarkably higher levels of most proinflammatory  
265 cytokines tested and small difference in some anti-inflammatory cytokines than VLP-SPAC<sub>G614</sub>  
266 or SPAC<sub>wt</sub> in human MDMs and MDDCs.

## 267 **DISCUSSION**

268 The SARS-CoV-2 Delta variant has higher transmissibility and thus has become the predominant  
269 strain worldwide in 2021(Li et al., 2021). It is important to understand the mechanisms of the  
270 increased transmissibility and cytokine release triggered by this variant. In this study, we  
271 investigated the cleavage and maturation efficiency of the Delta variant Spike protein (SP $\Delta$ C<sub>Delta</sub>)  
272 during pseudovirus assembly and its impact on cell-free pseudovirus infection and cell-cell  
273 fusion activities. The results demonstrated enhanced cleavage and maturation of SP $\Delta$ C<sub>Delta</sub> in the  
274 produced viral particles. Additionally, the studies clearly showed that SP $\Delta$ C<sub>Delta</sub> mediated more  
275 efficient pseudovirus infection and mediated a significantly enhanced cell-cell fusion process.  
276 Furthermore, our analyses revealed that SP<sub>Delta</sub>-PVLPs had stronger effects on stimulating NF- $\kappa$ B  
277 and AP-1 signaling in THP1 cells and elevated the production of several essential  
278 proinflammatory cytokines by human MDMs and MDDCs, compared with SP<sub>WT</sub>-PVLPs.

279 SARS-CoV-2 transmission and pathogenesis require the polybasic cleavage site between  
280 S1 and S2 in its SP (Johnson et al., 2021; Peacock et al., 2021a). This furin protease cleavable  
281 site is critical for the maturation of SARS-CoV-2 and its biological functions (Boson et al., 2021;  
282 Hoffmann et al., 2018; Hoffmann et al., 2020a). In an attempt to understand the mechanisms by  
283 which the Delta variant is more infectious than other variants, our study revealed that SP $\Delta$ C<sub>Delta</sub>  
284 was significantly more efficient in the processing of the precursor S into S1 and S2 compared  
285 with SP $\Delta$ C<sub>WT</sub> and SP $\Delta$ C<sub>G614</sub> in both the cells and PVPs. In the PVPs, the majority of SP $\Delta$ C<sub>Delta</sub>  
286 was presented as mature forms (S1 and S2), while some portions of the precursor S of SP $\Delta$ C<sub>WT</sub>  
287 and SP $\Delta$ C<sub>G614</sub> were still present in the PVPs (Fig. 1C, right panel). To further investigate the  
288 importance of the furin cleavage site for the enhanced cleavage of the Delta variant, we produced  
289 SP $\Delta$ C<sub>Delta</sub>-PVPs packaged in the presence or absence of the furin protease inhibitor CMK. As

290 expected, CMK significantly inhibited the cleavage of the spike protein of the Delta variant.

291         Among the mutations in the Delta variant spike protein, an amino acid proline (P681) at  
292 the N-terminus of the polybasic cleavage site (RRAR) was changed to arginine (R), known as the  
293 P681R mutation (Saito et al., 2021). The P681R mutation is of great importance because it is part  
294 of a proteolytic cleavage site for furin and furin-like proteases. The P618R mutation clearly plays  
295 a critical role in the SP of the Delta variant to abrogate host *O*-glycosylation (Zhang et al.,  
296 2021b). To further investigate whether this altered polybasic cleavage site (RRRAR) is required  
297 for effective furin cleavage of SARS-CoV-2 SP, we reverted the arginine (R) of 681 and  
298 asparagine (N) of 950 back to the original proline (P) and aspartic acid (D) on SP of the Delta  
299 variant (SPAC<sub>Delta-PD</sub>). The WB results showed that the cleavage of the SPAC<sub>Delta-PD</sub>-PVPs was  
300 comparable to that of SPAC<sub>WT</sub>-, SPAC<sub>G614</sub>- or SPAC<sub>Delta</sub>-PVPs produced in the presence of  
301 CMK. Consistent with other reports (Peacock et al., 2021b; Saito et al., 2021), our results further  
302 demonstrated that the P618R mutation in SPAC<sub>Delta</sub> is essential for the enhanced furin cleavage  
303 of Delta variant SP. Meanwhile, we also observed that S1 of SPAC<sub>Delta</sub> appeared to migrate faster  
304 than S1 of SPAC<sub>WT</sub> and SPAC<sub>G614</sub>. Although the mechanism is currently unknown, it could be  
305 related to the possible altered glycosylation content of SPAC<sub>Delta</sub> because a previous study  
306 revealed that P681R could circumvent host *O*-glycosylation (Zhang et al., 2021b). In addition,  
307 multiple amino acid mutations and deletions present in S1 of Delta SP may also partially  
308 contribute to this alteration. More detailed studies are required to analyze the possible underlying  
309 mechanism(s).

310         In this study, we also observed that SPAC<sub>Delta</sub> enhanced cell-free pseudovirus infection in  
311 A549<sub>ACE2+</sub> and Calu-3 cell lines and macrophages, indicating that SPAC<sub>Delta</sub> is an important  
312 factor contributing to the increased infectiousness of the Delta variant. Additionally, it was

313 observed that the infection mediated by SPAC<sub>Delta</sub>-pseudovirus was only slightly higher than that  
314 mediated by SPAC<sub>G614</sub>-pseudovirus, suggesting that the G614 mutation present in SP<sub>Delta</sub> may be  
315 one of the main driving forces for the increased infectivity of the Delta virus (Daniloski et al.,  
316 2020; Zhang et al., 2020). This finding is in agreement with previous studies showing that the  
317 D614G mutation in SARS-CoV-2 SP contributes immensely to virus infectivity and replication  
318 (Daniloski et al., 2020; Zhang et al., 2020). It should be noted that our results were based on  
319 single-cycle SPAC-pseudovirus replication; thus, the infection advantage of the native SARS-  
320 CoV-2 Delta variant needs further investigation.

321 It is well known that spike protein expressed at the surface of infected cells is sufficient  
322 to generate fusion with neighboring cells. Here, we further showed that significantly enhanced  
323 syncytia formation was observed when SPAC<sub>Delta</sub>-expressing 293T or A549 cells were cocultured  
324 with A549<sub>ACE2</sub> cells. This observation raised potential importance in terms of the SARS-CoV-2  
325 Delta variant's virulence since cell-to-cell fusion may provide another efficient method of viral  
326 dispersal in the host, thus indicating its stronger transmission among the population, as described  
327 previously (Michael Rajah et al., 2021). This finding is in agreement with recent reports that  
328 B.1.617.2 SP mediates highly efficient syncytia formation compared with wild-type SP (Michael  
329 Rajah et al., 2021; Mlcochova et al., 2021; Planas et al., 2021; Zhang et al., 2021a). Moreover,  
330 this efficient cell-to-cell transmission ability of SPAC<sub>Delta</sub> may enhance its resistance to host  
331 immune responses, such as antibody-mediated neutralization (Mlcochova et al., 2021; Planas et  
332 al., 2021). It is worth noting that we did not investigate the impact of TMPRSS2 on the cell-cell  
333 fusion process. For SARS-CoV-2, cleavage of S by furin at the S1/S2 site is required for  
334 subsequent cleavage by TMPRSS2 at the S2' site. Previous studies have demonstrated that  
335 TMPRSS2 could enhance the infectivity and fusogenic activity of different coronaviruses,

336 including SARS-CoV-2 (Buchrieser et al., 2020; Glowacka et al., 2011; Kleine-Weber et al.,  
337 2018; Matsuyama et al., 2010). Future investigations into the role of TMPRSS2 in SP Delta-  
338 induced syncytia formation and infection will provide a better understanding of the persistence,  
339 dissemination, and immune or inflammatory responses of Delta variants.

340 The severity of COVID-19 is highly correlated with dysregulated and excessive release  
341 of proinflammatory cytokines (Huang et al., 2020a). Hence, we also tested whether macrophages  
342 or dendritic cells act as major modulators of the immune response by producing a large amount  
343 of cytokines and chemokines to recruit immune cells and presenting antigens to them. The  
344 engagement of the spike protein of SARS-CoV-2 with the receptor ACE2 on THP1-derived  
345 macrophages is reported to initiate signaling pathways and activate the production of  
346 proinflammatory cytokines, including IL-6, TNF- $\alpha$ , and MIP1a (Pantazi et al., 2021). Here, we  
347 showed that NF $\kappa$ B and AP1 signaling pathway activities were also enhanced by SP $\Delta$ C<sub>Delta</sub>  
348 compared with SP $\Delta$ C<sub>WT</sub> in THP1 cells and THP1-derived macrophages, suggesting that  
349 SP $\Delta$ C<sub>Delta</sub> might promote the inflammatory status of these cells. Similarly, the SP of SARS-CoV-  
350 1 has been discovered to activate NF- $\kappa$ B and stimulate the release of IL-6 and TNF- $\alpha$  (Wang et  
351 al., 2007).

352 A previous study reported that high plasma levels of TNF $\alpha$ , IL-1, IL-6, IL-8 and other  
353 inflammatory mediators were found in severe COVID-19 patients, and the serum IL-6, IL-8 and  
354 TNF- $\alpha$  levels were strong and independent predictors of disease progression, severity and death.  
355 (Del Valle et al., 2020; Huang et al., 2020a; Santa Cruz et al., 2021). Interestingly, we found that  
356 SP $\Delta$ C<sub>Delta</sub> significantly enhanced the expression of several proinflammatory cytokines (TNF- $\alpha$ ,  
357 IL-1 $\beta$ , and IL-6) in both MDMs and MDDCs (Fig. 5). Especially for MDDCs, increased levels  
358 of other proinflammatory cytokines, including IFN- $\gamma$ , IL-2, IL-8, and IL-12p70 were also



359 detected (Fig. 5). However, SP $\Delta$ C<sub>wt</sub> only exhibited induction of IFN- $\gamma$  in MDDCs, but did not  
360 show any effect on other cytokine production of MDMs or MDDCs. This is agree with previous  
361 study that revealed, upon SARS-CoV-2 infection, neither macrophage, nor dendritic cells  
362 produce the pro-inflammatory cytokines (Niles et al., 2021). Mutations in Delta SP seem to be  
363 the key points that cause the differential expression of cytokines. Given the fact that IFN- $\gamma$ ,  
364 TNF- $\alpha$ , IL-1 $\beta$  and IL-12 are T-helper-1 (Th1) cytokines, it also suggests that the Th1/Th2  
365 balance has further shifted to Th1 dominance after stimulation with SP $\Delta$ C<sub>Delta</sub>-PVLP. Along with  
366 proinflammatory cytokines, three anti-inflammatory cytokines (IL-4, IL-10 and IL-13) were also  
367 increased in SP $\Delta$ C<sub>Delta</sub>-PVLP treated macrophages compared with SP $\Delta$ C<sub>WT</sub>-PVLP.treated  
368 macrophages. Consistently, higher secretion of T-helper-2 (Th2) cytokines such as IL-4 and IL-  
369 10 has been reported in ICU patients than in non-ICU patients (Huang et al., 2020a). Their  
370 functions are to suppress both inflammation and the TH1 cellular response, indicating that the  
371 balances between pro- and anti-inflammation, as well as the balances between TH1 and TH2  
372 cellular responses existing in patients, are important for the clinical outcomes of COVID-19  
373 therapy. However, the lower IL-10 level in all PVLPs treated MDDCs is surprising and the  
374 reason of this is unclear. In conclusion, SP $\Delta$ C<sub>Delta</sub>-treated macrophages and DCs are in a higher  
375 inflammatory state and in a Th1-dominant Th1/Th2 balance.

376 Overall, we demonstrated that the SARS-CoV-2 Delta variant spike protein exhibited  
377 enhanced cleavage and maturation, which may play an important role in viral infection and cell-  
378 cell transmission. Furthermore, we revealed that SP<sub>Delta</sub> had stronger effects on stimulating NF-  
379  $\kappa$ B and AP-1 signaling in monocytes and the release of proinflammatory cytokines from human  
380 macrophages and dendritic cells. All of these studies provide strong evidence to support the  
381 important role of Delta SP during virus infection, transmission and pathogenesis.

382

## 383 **MATERIALS AND METHODS**

### 384 **Plasmid constructs**

385 The SARS-CoV-2 SP protein-expressing plasmids (pCAGGS-nCoVSP $\Delta$ C and pCAGGS-  
386 nCoVSP $\Delta$ C<sub>G614</sub>) were described previously (Ao et al., 2021a). The gene encoding SP $\Delta$ C<sub>Delta</sub> or  
387 SP $\Delta$ C<sub>Delta-PD</sub> was synthesized (Genescript) and cloned into the pCAGGS plasmid, and each  
388 mutation was confirmed by sequencing. pEF1-SP $\Delta$ Cwt, pEF1-SP $\Delta$ C<sub>G614</sub> or pEF1-SP $\Delta$ C<sub>Delta</sub> was  
389 constructed by inserting the cDNA encoding SP $\Delta$ Cwt, SP $\Delta$ C<sub>G614</sub> or SP $\Delta$ C<sub>Delta</sub> through the *Bam*HI  
390 and *Nhe*I sites into the pEF1-pcs-puro vector (Ao et al., 2008). The HIV RT/IN/Env trideleted  
391 proviral plasmid containing the Gaussia luciferase gene ( $\Delta$ RI/E/Gluc) and the helper packaging  
392 plasmid pCMV $\Delta$ 8.2 encoding the HIV Gag-Pol plasmids have been described previously (Ao et  
393 al., 2016; Zhang et al., 2016).

394

### 395 **Cell culture, antibodies and chemicals**

396 Human embryonic kidney cells (HEK293T), human lung (carcinoma) cells (A549), A549<sub>ACE2</sub>,  
397 Calu-3 cells and THP1- sensor cells were cultured in Dulbecco's modified Eagle's medium or  
398 RPMI 1640 medium supplemented with 10% fetal bovine serum (F.B.S.) and 1%  
399 penicillin/streptomycin. To obtain human MDMs or MDDCs, human peripheral blood  
400 mononuclear cells (hPBMCs) from healthy donors were collected by sedimentation on a Ficoll  
401 (Lymphoprep; Axis-Shield) gradient, adherent to 24-well plates for 2 hrs, and then treated with  
402 macrophage colony stimulator (M-CSF) or granulocyte-macrophage-stimulating factor (GM-  
403 CSF) and IL-4 (R&D system) for 7 days.

404 The THP1-NF- $\kappa$ B-Luc and THP1-AP-1-Luc sensor cell lines were described previously (Ao et  
405 al., 2021b). To obtain THP1-derived macrophages, THP-1-NF- $\kappa$ B-Luc and THP1-AP-1-Luc

406 sensor cell lines were treated with phorbol 12-myristate 13-acetate (PMA) (200 ng/mL) for 3  
407 days followed by 2 days of rest, as previously described (Starr et al., 2018). A549-expressing  
408 human ACE2 (A549<sub>ACE2</sub>) cells were generated by transducing A549 cells with the ACE2-  
409 expressing lentiviral vector (pLenti-C-mGFP-ACE2) (Origene, Cat# PS100093) and then  
410 selected with puromycin according to the manufacturer's procedure.

411 The rabbit polyclonal antibody against SARS-CoV-2 SP/RBD (Cat# 40592-T62) or human  
412 SARS-CoV-2 S-NTD antibody (E-AB-V1030) was obtained from Sino Biological or  
413 Elabscience. Mouse monoclonal antibody (1A9) against SARS-CoV-2 SP-S2 (Cat# ab273433)  
414 was obtained from Abcam. Anti-HIVp24 monoclonal antibody was described previously (Ao et  
415 al., 2007; Qiu et al., 2011). Anti-human ACE2 antibody (sc-390851) was obtained from Santa  
416 Cruz Biotechnology Inc. Furin inhibitor I, a peptidyl chloromethylketone (CMK) (Cat# 344930),  
417 was obtained from Millipore Sigma.

418

#### 419 **Virus production and infection experiments**

420 SARS-CoV-2 SPΔC pseudotyped viruses (CoV-2-SPΔC-PVs, CoV-2-SPΔC<sub>G614</sub>-PVs and CoV-  
421 2-SPΔC<sub>Delta</sub>-PVs) or pseudotyped virus-like particles (VLPs) were produced by transfecting  
422 HEK293T cells with pCAGGS-SPΔC<sub>WT</sub>, pCAGGS-SPΔC<sub>G614</sub> or pCAGGS-SPΔC<sub>Delta</sub> and  
423 pCMVΔ8.2 with or without a Gluc-expressing HIV vector ΔRI/E/Gluc (Ao et al., 2021a). After  
424 48 hrs of transfection, cell culture supernatants were collected, and VPs or VLPs were purified  
425 from the supernatant by ultracentrifugation (32,000 rpm) for 2 hrs. The pelleted VPs or VLPs  
426 were resuspended in RPMI medium, and virus titers were quantified by HIV-1 p24 amounts  
427 using an HIV-1 p24 ELISA.

428 To measure the infection ability of SARS-CoV-2 SP $\Delta$ C pseudotyped VPs, equal amounts of each  
429 SP $\Delta$ C-PVs stock (as adjusted by p24 levels) were used to infect A549<sub>ACE2</sub>, Calu-3 cells, human  
430 MDMs or MDDCs. After different time intervals (24, 48 and 72 hrs), the supernatants were  
431 collected, and the viral infection levels were monitored by measuring Gaussia luciferase (Gluc)  
432 activity. Briefly, 50  $\mu$ l of coelenterazine substrate (Nanolight Technology) was added to 10  $\mu$ l of  
433 supernatant, mixed well and read in a luminometer (Promega, U.S.A.).

434 To evaluate the effects of various SCoV-2 SP $\Delta$ C-VLPs on the NF- $\kappa$ B and AP-1 signaling  
435 pathways, the same amount of each SP $\Delta$ C-pseudotyped VLP stock (10 ng, as adjusted by the p24  
436 levels) was directly added to THP1-NF- $\kappa$ B-Luc or THP1-AP1-Luc sensor cells. After 6 hrs, the  
437 cells were collected and subjected to luciferase assay as described previously (Ao et al., 2021b).

438 To test the effect of different SP $\Delta$ C-VLPs on cytokine production in MDMs and MDDCs, the  
439 same amount of each SP $\Delta$ C-VP stock (20 ng, as adjusted by the p24 levels) was added to MDMs  
440 and MDDCs, and the supernatants were collected after 24 hrs. The cytokine (IFN- $\gamma$ , IL-1 $\beta$ , IL-2,  
441 IL-4, IL-6, IL-8, IL-10, IL-12p70, IL-13, TNF- $\alpha$ ) levels in the supernatants were measured using  
442 the MSD V-PLEX proinflammatory Panel 1 (human) Kit (MesoScale Discovery, USA, Cat#  
443 K15049D-1) following the manufacturer's procedure.

444

#### 445 **Generation of different SP $\Delta$ C-expressing A549 stable cell lines**

446 Production of lentiviral vectors expressing different SP $\Delta$ C: 293T cells were cotransfected with  
447 pEF1-SP $\Delta$ C<sub>wt</sub>, pEF1-SP $\Delta$ C<sub>G614</sub> or pEF1-SP $\Delta$ C<sub>Delta</sub> with packaging plasmid  $\Delta$ 8.2 and VSV-G  
448 expressing plasmid. Forty-eight hours posttransfection, each lentiviral vector particle in the  
449 supernatant was collected. Then, each produced lentiviral particle was used to transduce A549  
450 cells, and the transduced cells were selected with puromycin for one week. SP $\Delta$ C<sub>wt</sub>/mutant

451 expression in the different transduced A549 cells was evaluated by WB using an anti-RBD  
452 antibody.

453

#### 454 **Immunofluorescence assay**

455 293T cells transfected with various SARS-CoV-2 SP $\Delta$ C-expressing plasmids were grown on  
456 glass coverslips (12 mm<sup>2</sup>) in a 24-well plate. After 48 hrs, cells on the coverslip were fixed in 4%  
457 paraformaldehyde for 5 minutes and permeabilized with 0.2% Triton X-100 in PBS. The cells  
458 were then incubated with primary antibodies against the N-terminal domain of SARS-CoV-2 SP  
459 followed by the corresponding FITC-conjugated secondary antibodies. The cells were viewed  
460 under a computerized Axiovert 200 fluorescence microscope (ZEISS). ).

461

#### 462 **Syncytium formation assay**

463 293T cells were transfected with pCAGGS-SP $\Delta$ C<sub>WT</sub>, SP $\Delta$ C<sub>G614</sub>, SP $\Delta$ C<sub>Delta</sub> or SP $\Delta$ C<sub>DeltaPD</sub>  
464 plasmids using Lipofectamine 2000. After 24 hrs, the cells were washed, resuspended and mixed  
465 with A549<sub>ACE2</sub> cells at a 1:3 ratio and plated into 48-well plates. For syncytium formation of the  
466 stable cell line, A549-SP $\Delta$ C<sub>WT</sub> or A549-SP $\Delta$ C<sub>Delta</sub> cells were detached with 0.05% trypsin and  
467 mixed with A549 or A549<sub>ACE2</sub> cells. At different time points, syncytium formation was observed,  
468 counted and imaged by bright-field microscopy (Axiovert 200, ZEISS).

469

#### 470 **Statistics**

471 Statistical analysis of cytokine levels, including the results of GLuc assay, Luciferase assay, and  
472 various cytokine/chemokines assay, were performed using the unpaired t-test (considered  
473 significant at P $\geq$ 0.05) by GraphPad Prism 9 software.

474 **ACKNOWLEDGEMENTS**

475 We thank Dr. Darwyn Kobasa for providing the Calu-3 cell lines and technique supports.  
476 Titus Olukitibi is a recipient of the University Manitoba Graduate scholarship. This work was  
477 supported by Canadian 2019 Novel Coronavirus (COVID-19) Rapid Research Funding (OV5-  
478 170710) by Canadian Institute of Health Research (CIHR) and Research Manitoba, and CIHR  
479 COVID-19 Variant Supplement grant (VS1-175520) to X-J.Y. This work was also supported  
480 by the Manitoba Research Chair Award from the Research Manitoba (RM) to to X-J.Y.

481

482 **AUTHOR CONTRIBUTIONS**

483 Experimental design, X. Y, Z.A. and M.J.O; Investigation, Z.A., M.J.O., and O.T.A; Writing-  
484 Original Draft Preparation, Z.A. and M. J. O. and O.T.A; Review, Z.A. M. J. O. and X.Y.  
485 Supervision, X.Y.

486

487 **DECLARATION OF INTERESTS**

488 The authors declare no competing interests.

489

490

491

## 492 REFERENCES

- 493
- 494 Ao, Z., Huang, G., Yao, H., Xu, Z., Labine, M., Cochrane, A.W., and Yao, X. (2007). Interaction of human  
495 immunodeficiency virus type 1 integrase with cellular nuclear import receptor importin 7 and its impact  
496 on viral replication. *Journal of Biological Chemistry* 282, 13456-13467.
- 497 Ao, Z., Huang, J., Tan, X., Wang, X., Tian, T., Zhang, X., Ouyang, Q., and Yao, X. (2016). Characterization of  
498 the single cycle replication of HIV-1 expressing Gaussia luciferase in human PBMCs, macrophages, and in  
499 CD4(+) T cell-grafted nude mouse. *Journal of virological methods* 228, 95-102.
- 500 Ao, Z., Yu, Z., Wang, L., Zheng, Y., and Yao, X. (2008). Vpr14-88-Apobec3G fusion protein is efficiently  
501 incorporated into Vif-positive HIV-1 particles and inhibits viral infection. *PloS one* 3, e1995.
- 502 Ao, Z.-j., Chan, M., Ouyang, M., Abiola, T., Mahmoudi, M., Kobasa, D., and Yao, X.-J. (2021a).  
503 Identification and evaluation of the inhibitory effect of *Prunella vulgaris* extract on SARS-coronavirus 2  
504 virus entry. *PloS one*, <https://doi.org/10.1371/journal.pone.0251649>
- 505 Ao, Z.-j., Wang, L.-j., Azizi, H., Olukitibi, T., Mahmoudi, M., Kobinger, G., and Yao, X.-j. (2021b).  
506 Development and Evaluation of an Ebola Virus Glycoprotein Mucin-Like Domain Replacement System as  
507 a New Dendritic Cell-Targeting Vaccine Approach against HIV-1. *Journal of virology* 95, e0236820. PMID:  
508 34011553.
- 509 Banu, S., Jolly, B., Mukherjee, P., Singh, P., Khan, S., Zaveri, L., Shambhavi, S., Gaur, N., Reddy, S., and  
510 Kaveri, K. (2020). A Distinct Phylogenetic Cluster of Indian Severe Acute Respiratory Syndrome  
511 Coronavirus 2 Isolates. Paper presented at: Open forum infectious diseases (Oxford University Press US).
- 512 Bertram, S., Dijkman, R., Habjan, M., Heurich, A., Gierer, S., Glowacka, I., Welsch, K., Winkler, M.,  
513 Schneider, H., and Hofmann-Winkler, H. (2013). TMPRSS2 activates the human coronavirus 229E for  
514 cathepsin-independent host cell entry and is expressed in viral target cells in the respiratory epithelium.  
515 *Journal of virology* 87, 6150-6160.
- 516 Boson, B., Legros, V., Zhou, B., Siret, E., Mathieu, C., Cosset, F.-L., Lavillette, D., and Denolly, S. (2021).  
517 The SARS-CoV-2 envelope and membrane proteins modulate maturation and retention of the spike  
518 protein, allowing assembly of virus-like particles. *Journal of Biological Chemistry* 296.
- 519 Boumaza, A., Gay, L., Mezouar, S., Bestion, E., Diallo, A.B., and Michel, M.e.a. (2021). Monocytes and  
520 macrophages, targets of SARS-CoV-2: the clue for Covid-19 immunoparalysis. *J Infect Dis* *doi:*  
521 *10.1093/infdis/jiab044*.
- 522 Buchrieser, J., Dufloo, J., Hubert, M., Monel, B., Planas, D., Rajah, M.M., and al, e. (2020). Syncytia  
523 formation by SARS-CoV-2-infected cells. *The EMBO journal* 39.  
524 *e106267*<https://doi.org/10.15252/embj.2020106267>.
- 525 Bussania, R., Schneider, E., Zentilinb, L., Collesi, C., Ali, H., and al., e. (2020). Persistence of viral RNA,  
526 pneumocyte syncytia and thrombosis are hallmarks of advanced COVID-19 pathology. *EBioMedicine* 61,  
527 103104.
- 528 Cattin-Ortolá, J., Welch, L., Maslen, S.L., Skehel, J.M., Papa, G., James, L.C., and Munro, S. (2020).  
529 Sequences in the cytoplasmic tail of SARS-CoV-2 Spike facilitate expression at the cell surface and  
530 syncytia formation. *bioRxiv* <https://doi.org/10.1101/2020.10.12.335562>.
- 531 CDC (2021). SARS-CoV-2 Variant Classifications and Definitions. Centers for Disease Control and  
532 Prevention [https://http://www.cdc.gov/coronavirus/2019-ncov/variants/variant-](https://http://www.cdc.gov/coronavirus/2019-ncov/variants/variant-info.html?CDC_AA_refVal=https%3A%2F%2Fwww.cdc.gov%2Fcoronavirus%2F2019-ncov%2Fcases-updates%2Fvariant-surveillance%2Fvariant-info.html)  
533 [info.html?CDC\\_AA\\_refVal=https%3A%2F%2Fwww.cdc.gov%2Fcoronavirus%2F2019-ncov%2Fcases-](https://http://www.cdc.gov/coronavirus/2019-ncov/variants/variant-info.html?CDC_AA_refVal=https%3A%2F%2Fwww.cdc.gov%2Fcoronavirus%2F2019-ncov%2Fcases-updates%2Fvariant-surveillance%2Fvariant-info.html)  
534 [updates%2Fvariant-surveillance%2Fvariant-info.html](https://http://www.cdc.gov/coronavirus/2019-ncov/variants/variant-info.html?CDC_AA_refVal=https%3A%2F%2Fwww.cdc.gov%2Fcoronavirus%2F2019-ncov%2Fcases-updates%2Fvariant-surveillance%2Fvariant-info.html).
- 535 Cherian, S., Potdar, V., Jadhav, S., Yadav, P., Gupta, N., Das, M., Rakshit, P., Singh, S., Abraham, P., and  
536 Panda, S. (2021). Convergent evolution of SARS-CoV-2 spike mutations, L452R, E484Q and P681R, in the  
537 second wave of COVID-19 in Maharashtra, India. *bioRxiv*.

538 Coutard, B., Valle, C., de Lamballerie, X., Canard, B., Seidah, N.G., and Decroly, E. (2020). The spike  
539 glycoprotein of the new coronavirus 2019-nCoV contains a furin-like cleavage site absent in CoV of the  
540 same clade. *Antiviral research* 176, 104742.

541 Daniloski, Z., Jordan, T.X., Ilmain, J.K., Guo, X., Bhabha, G., and Sanjana, N.E. (2020). The Spike D614G  
542 mutation increases SARS-CoV-2 infection of multiple human cell types. *Elife* 10, e65365.

543 Del Valle, D.M., Kim-Schulze, S., Huang, H.-H., and Beckmann, N.D.e.a. (2020). An inflammatory cytokine  
544 signature predicts COVID-19 severity and survival. *nature medicine* 26, 1636–1643.

545 Galloway, S.E., Paul, P., MacCannell, D.R., Johansson, M.A., Brooks, J.T., MacNeil, A., Slayton, R.B., Tong,  
546 S., Silk, B.J., and Armstrong, G.L. (2021). Emergence of SARS-CoV-2 b. 1.1. 7 lineage in the United States,  
547 December 29, 2020–January 12, 2021. *Morbidity and Mortality Weekly Report* 70, 95.

548 Glowacka, I., Bertram, S., Müller, M.A., Allen, P., and Soilleux, E.e.a. (2011). Evidence that TMPRSS2  
549 activates the severe acute respiratory syndrome coronavirus spike protein for membrane fusion and  
550 reduces viral control by the humoral immune response. *Journal of virology* 85, 4122-4134.

551 Greaney, A.J., Starr, T.N., Gilchuk, P., Zost, S.J., Binshtein, E., Loes, A.N., Hilton, S.K., Huddleston, J.,  
552 Eguia, R., and Crawford, K.H.D. (2021). Complete mapping of mutations to the SARS-CoV-2 spike  
553 receptor-binding domain that escape antibody recognition. *Cell host & microbe* 29, 44-57. e49.

554 Hadjadj, J.r.m., Yatim, N., Barnabei, L., Corneau, A.I., Boussier, J., Smith, N.a., PÅra, H., Charbit, B.,  
555 Bondet, V., and Chenevier-Gobeaux, C. (2020). Impaired type I interferon activity and inflammatory  
556 responses in severe COVID-19 patients. *Science* 369, 718-724.

557 Hoffmann, M., Hofmann-Winkler, H., and Pahlmann, S. (2018). Priming time: how cellular proteases arm  
558 coronavirus spike proteins. In *Activation of Viruses by Host Proteases* (Springer), pp. 71-98.

559 Hoffmann, M., Kleine-Weber, H., and Pahlmann, S. (2020a). A multibasic cleavage site in the spike  
560 protein of SARS-CoV-2 is essential for infection of human lung cells. *Molecular cell* 78, 779-784. e775.

561 Hoffmann, M., Kleine-Weber, H., Schroeder, S., KrÅ¼ger, N., Herrler, T., Erichsen, S., Schiergens, T.S.,  
562 Herrler, G., Wu, N.-H., and Nitsche, A. (2020b). SARS-CoV-2 cell entry depends on ACE2 and TMPRSS2  
563 and is blocked by a clinically proven protease inhibitor. *cell* 181, 271-280. e278.

564 Hojyo, S., Uchida, M., Tanaka, K., Hasebe, R., Tanaka, Y., Murakami, M., Hirano, T., and (2020). How  
565 COVID-19 induces cytokine storm with high mortality. *Inflammation and Regeneration* 40, 37.

566 Huang, C.L., Wang, Y.M., Li, X.W., Ren, L., Zhao, J.P., Yi Hu, Y., and al., e. (2020a). Clinical features of  
567 patients infected with 2019 novel coronavirus in Wuhan, China. *THE LANCET* 395, 497-506.

568 Huang, Y., Yang, C., Xu, X.-f., Xu, W., and Liu, S.-w. (2020b). Structural and functional properties of SARS-  
569 CoV-2 spike protein: potential antiviral drug development for COVID-19. *Acta Pharmacologica Sinica* 41,  
570 1141-1149.

571 Johnson, B.A., Xie, X., Kalveram, B., Lokugamage, K.G., Muruato, A., Zou, J., Zhang, X., Juelich, T., Smith,  
572 J.K., and Zhang, L. (2020). Furin cleavage site is key to SARS-CoV-2 pathogenesis. *bioRxiv*.

573 Johnson, B.A., Xuping Xie, X.p., Kalveram, B., and Lokugamage, K.G., et al. (2021). Loss of furin cleavage  
574 site attenuates SARS-CoV-2 pathogenesis. *Nature* 591, 293-299.

575 Kawasaki, T., and Kawai, T. (2014). Toll-like receptor signaling pathways. *Front Immunol*  
576 <https://doi.org/10.3389/fimmu.2014.00461>.

577 Kleine-Weber, H., Elzayat, M.T., Hoffmann, M., and Pöhlmann, S. (2018). Functional analysis of potential  
578 cleavage sites in the MERS-coronavirus spike protein. *Scientific reports* 8, 16597

579 Li, B., Deng, A., Li, K., Hu, Y., Li, Z., Xiong, Q., Liu, Z., Guo, Q., Zou, L., and Zhang, H. (2021). Viral infection  
580 and transmission in a large well-traced outbreak caused by the Delta SARS-CoV-2 variant. *MedRxiv*.  
581 <https://doi.org/10.1101/2021.07.07.21260122>

582 Liu, Y., Liu, J.Y., Johnson, B.A., Xia, H.J., Ku, Z.Q., and al., e. (2021). Delta spike P681R mutation enhances  
583 SARS-CoV-2 fitness over Alpha variant. *BioRxiv* doi: 10.1101/2021.08.12.456173. .



584 Matsuyama, S., Nagata, N., Shirato, K., Kawase, M., Takeda, M., and Taguchi, F. (2010). Efficient  
585 activation of the severe acute respiratory syndrome coronavirus spike protein by the transmembrane  
586 protease TMPRSS2. *Journal of virology* *84*, 12658-12664.

587 McCallum, M., Walls, A.C., Sprouse, K.R., Bowen, J.E., Rosen, L.E., Dang, H.V., Marco, A.D., Franko, N.,  
588 Tilles, S.W., Logue, J., *et al.* Molecular basis of immune evasion by the Delta and Kappa SARS-CoV-2  
589 variants. *Science* *0*, eabl8506.

590 Mehta, P., McAuley, D.F., Brown, M., Sanchez, E., Tattersall, R.S., and Manson, J.J. (2020). COVID-19:  
591 consider cytokine storm syndromes and immunosuppression. *The Lancet* *395*, 1033-1034.

592 Michael Rajah, M., Hubert, M., Bishop, E., Saunders, N., Robinot, R., Grzelak, L., Planas, D., Dufloo, J.,  
593 Gellenoncourt, S., and Bongers, A. (2021). SARS-CoV2 Alpha, Beta and Delta variants display enhanced  
594 Spike-mediated Syncytia Formation. *The EMBO Journal*, e108944.

595 Mlcochova, P., Kemp, S.A., Dhar, M.S., Papa, G., Meng, B., Ferreira, I.A.T.M., Datir, R., Collier, D.A.,  
596 Albecka, A., and Singh, S. (2021). SARS-CoV-2 B. 1.617. 2 Delta variant replication and immune evasion.  
597 *Nature*, 1-6.

598 Neufeldt, C.J., Cerikan, B., Cortese, M., Frankish, J., Lee, J.-Y., Plociennikowska, A., Heigwer, F., Joecks, S.,  
599 Burkart, S.S., Zander, D.Y., *et al.* (2020a). SARS-CoV-2 infection induces a pro-inflammatory cytokine  
600 response through cGAS-STING and NF- $\kappa$ B. *bioRxiv*, 2020.2007.2021.212639.

601 Neufeldt, C.J., Cerikan, B., Cortese, M., Frankish, J., and Lee, J.-Y.e.a. (2020b). SARS-CoV-2 infection  
602 induces a pro-inflammatory cytokine response through cGAS-STING and NF- $\kappa$ B *bioRxiv*  
603 <https://doi.org/10.1101/2020.07.21.212639>.

604 Niles, M.A., Gogesch, P., Kronhart, S., Ortega Iannazzo, S., Kochs, G., Waibler, Z., and Anzaghe, M.  
605 (2021). Macrophages and Dendritic Cells Are Not the Major Source of Pro-Inflammatory Cytokines Upon  
606 SARS-CoV-2 Infection. *Frontiers in Immunology* *12*.

607 Nonaka, C.K.V., Franco, M.M., Grãxf, T., Mendes, A.V.A., de Aguiar, R.S., Giovanetti, M., and de Freitas  
608 Souza, B.S. (2021). Genomic Evidence of a Sars-Cov-2 Reinfection Case With E484K Spike Mutation in  
609 Brazil.

610 Paiva, M.H.S., Guedes, D.R.D., Docena, C.s., Bezerra, M.F., Dezordi, F.Z., Machado, L.C., Krovovsky, L.,  
611 Helvecio, E., da Silva, A.F., and Vasconcelos, L.R.S. (2021). Multiple introductions followed by ongoing  
612 community spread of SARS-CoV-2 at one of the largest metropolitan areas of Northeast Brazil. *Viruses*  
613 *12*, 1414.

614 Pantazi, I., Al-Qahtani, A.A., Alhamlan, F.S., H., A., Matou-Nasri, S., George Sourvinos, G., Eleni Vergadi,  
615 E., and Christos Tsatsanis, C. (2021). SARS-CoV-2/ACE2 Interaction Suppresses IRAK-M Expression and  
616 Promotes Pro-Inflammatory Cytokine Production in Macrophages. *Front Immunol* *12*.

617 Patra, T., Meyer, K., Geerling, L., Isbell, S., F., D., Hoft, D.F., Brien, J., Pinto, A.K., B., R., Ray, R.B., *et al.*  
618 (2020). SARS-CoV-2 spike protein promotes IL-6 trans-signaling by activation of angiotensin II receptor  
619 signaling in epithelial cells. *PLoS Pathogens*, <https://doi.org/10.1371/journal.ppat.1009128>

620 Peacock, T.P., Goldhill, D.H., Zhou, J., Baillon, L., and al., e. (2021a). The furin cleavage site in the SARS-  
621 CoV-2 spike protein is required for transmission in ferrets. *Nat Microbiol* *6*, 899-909.

622 Peacock, T.P., Sheppard, C.M., Brown, J.C., Goonawardane, N., Zhou, J., Whiteley, M., de Silva, T.I.,  
623 Barclay, W.S., and Consortium, P.H.E.V. (2021b). The SARS-CoV-2 variants associated with infections in  
624 India, B. 1.617, show enhanced spike cleavage by furin. *bioRxiv*.

625 Planas, D., Veyer, D., Baidaliuk, A., Staropoli, I., Guivel-Benhassine, F., Rajah, M.M., Planchais, C., Porrot,  
626 F.o., Robillard, N., and Puech, J. (2021). Reduced sensitivity of SARS-CoV-2 variant Delta to antibody  
627 neutralization. *Nature* *596*, 276-280.

628 Qiu, X., Alimonti, J.B., Melito, P.L., Fernando, L., Ströher, U., and Jones, S.M. (2011). Characterization of  
629 Zaire ebolavirus glycoprotein-specific monoclonal antibodies. *Clinical immunology* *141*, 218-227.

630 Ranjan, R., Sharma, A., and Verma, M.K. (2021). Characterization of the Second Wave of COVID-19 in  
631 India. *medRxiv*.

632 Reardon, S. (2021). How the Delta variant achieves its ultrafast spread. *Nature* 21.

633 Resende, P.C., Bezerra, J.o.F., Vasconcelos, R., Arantes, I., Appolinario, L., Mendonça, A.C., Paixao, A.C.,  
634 Rodrigues, A.C.D., Silva, T., and Rocha, A.S. (2021). Spike E484K mutation in the first SARS-CoV-2  
635 reinfection case confirmed in Brazil, 2020. *Virological* [Internet] 10.

636 Sahoo, J.P., Mishra, A.P., and Samal, K.C. (2021). Triple Mutant Bengal Strain (B. 1.618) of Coronavirus  
637 and the Worst COVID Outbreak in India. *Biotica Research Today* 3, 261-265.

638 Saito, A., Irie, T., Suzuki, R., Maemura, T., Nasser, H., Uriu, K., Kosugi, Y., Shirakawa, K., Sadamasu, K., and  
639 Kimura, I. (2021). SARS-CoV-2 spike P681R mutation, a hallmark of the Delta variant, enhances viral  
640 fusogenicity and pathogenicity. *bioRxiv*.

641 Santa Cruz, A., Mendes-Frias, A., I., O.A., Dias, L., A.R., M., and Carvalho, A. (2021). Interleukin-6 Is a  
642 Biomarker for the Development of Fatal Severe Acute Respiratory Syndrome Coronavirus 2 Pneumonia.  
643 *Front Immunol* <https://doi.org/10.3389/fimmu.2021.613422>.

644 Santos, J.C., and Passos, G.A. (2021). The high infectivity of SARS-CoV-2 B. 1.1. 7 is associated with  
645 increased interaction force between Spike-ACE2 caused by the viral N501Y mutation. *bioRxiv*,  
646 2020.2012. 2029.424708.

647 Srivastava, S., Banu, S., Singh, P., Sowpati, D.T., and Mishra, R.K. (2021). SARS-CoV-2 genomics: An Indian  
648 perspective on sequencing viral variants. *Journal of Biosciences* 46, 1-14.

649 Starr, T., Bauler, T.J., Malik-Kale, T., and Steele-Mortimer, O. (2018). The phorbol 12-myristate-13-  
650 acetate differentiation protocol is critical to the interaction of THP-1 macrophages with *Salmonella*  
651 *Typhimurium*. *PLoS one* <https://doi.org/10.1371/journal.pone.0193601>

652 Tegally, H., Wilkinson, E., Giovanetti, M., Iranzadeh, A., Fonseca, V., Giandhari, J., Doolabh, D., Pillay, S.,  
653 San, E.J., and Msoni, N. (2020). Emergence and rapid spread of a new severe acute respiratory  
654 syndrome-related coronavirus 2 (SARS-CoV-2) lineage with multiple spike mutations in South Africa.  
655 *medRxiv*.

656 Twohig, K.A., Nyberg, T., Zaidi, A., Thelwall, S., Sinnathamby, M.A., Aliabadi, S., and al., e. (2021).  
657 Hospital admission and emergency care attendance risk for SARS-CoV-2 delta (B.1.617.2) compared with  
658 alpha (B.1.1.7) variants of concern: a cohort study. *THE LANCET Infectious Diseases*  
659 *DOI:https://doi.org/10.1016/S1473-3099(21)00475-8*.

660 Volz, E., Mishra, S., Chand, M., Barrett, J.C., Johnson, R., Geidelberg, L., Hinsley, W.R., Laydon, D.J.,  
661 Dabrera, G., and Toole, A. (2021). Transmission of SARS-CoV-2 Lineage B. 1.1. 7 in England:  
662 Insights from linking epidemiological and genetic data. *medRxiv*, 2020.2012. 2030.20249034.

663 Wang, W., Ye, L.-B., Ye, L., Li, B.-Z., Gao, B., and al., e. (2007). Up-regulation of IL-6 and TNF-alpha  
664 induced by SARS-coronavirus spike protein in murine macrophages via NF-kappaB pathway. *Virus Res*  
665 128, 1-8.

666 WHO (2021). WHO Coronavirus (COVID-19) Dashboard. World Health Organization  
667 <https://covid19.who.int/>.

668 Worldometer (2021). COVID-19 Coronavirus Pandemic Worldometer  
669 <https://http://www.worldometers.info/coronavirus/>.

670 Xia, S., Lan, Q., Su, S., Wang, X., Xu, W., Liu, Z., Zhu, Y., Wang, Q., Lu, L., and Jiang, S. (2020). The role of  
671 furin cleavage site in SARS-CoV-2 spike protein-mediated membrane fusion in the presence or absence  
672 of trypsin. *Signal Transduction and Targeted Therapy* 5, 92.

673 Xu, Z.-S., Shu, T., Kang, L., Wu, D., Zhou, X., Liao, B.-W., Sun, X.-L., Zhou, X., and Wang, Y.-Y. (2020).  
674 Temporal profiling of plasma cytokines, chemokines and growth factors from mild, severe and fatal  
675 COVID-19 patients. *Signal transduction and targeted therapy* 5, 1-3.

676 Yang, L., Liu, S., Liu, J., Zhang, Z., Wan, X., Huang, B., Chen, Y., and Zhang, Y. (2020). COVID-19:  
677 immunopathogenesis and Immunotherapeutics. *Signal transduction and targeted therapy* 5, 1-8.

678 Zhang, J., Xiao, T., Cai, Y., Lavine, C.L., Peng, H., Zhu, H., Anand, K., Tong, P., Gautam, A., and Mayer, M.L.  
679 (2021a). Membrane fusion and immune evasion by the spike protein of SARS-CoV-2 Delta variant.  
680 *Science*, eabl9463.

681 Zhang, J., Xiao, T., Cai, Y., Lavine, C.L., Peng, H., Zhu, H., Anand, K., Tong, P., Gautam, A., Mayer, M.L., *et*  
682 *al.* Membrane fusion and immune evasion by the spike protein of SARS-CoV-2 Delta variant. *Science* *0*,  
683 eabl9463.

684 Zhang, L., Jackson, C.B., Mou, H., Ojha, A., Peng, H., Quinlan, B.D., Rangarajan, E.S., Pan, A.,  
685 Vanderheiden, A., and Suthar, M.S. (2020). SARS-CoV-2 spike-protein D614G mutation increases virion  
686 spike density and infectivity. *Nature communications* *11*, 1-9.

687 Zhang, L., Mann, M., Syed, Z., Reynolds, H.M., Tian, E., Samara, N.L., Zeldin, D.C., Tabak, L.A., and K.G.,  
688 T.H. (2021b). Furin cleavage of the SARS-CoV-2 spike is modulated by O-glycosylation. *PNAS* *118*,  
689 e2109905118.

690 Zhang, X., Ao, Z., Bello, A., Ran, X., Liu, S., Wigle, J., Kobinger, G., and Yao, X. (2016). Characterization of  
691 the inhibitory effect of an extract of *Prunella vulgaris* on Ebola virus glycoprotein (GP)-mediated virus  
692 entry and infection. *Antiviral research* *127*, 20-31.

693 Zhou, B., Thao, T.T.N., Hoffmann, D., Taddeo, A., Ebert, N., Labroussaa, F., Pohlmann, A., King, J., Steiner,  
694 S., and Kelly, J.N. (2021). SARS-CoV-2 spike D614G change enhances replication and transmission. *Nature*  
695 *592*, 122-127.

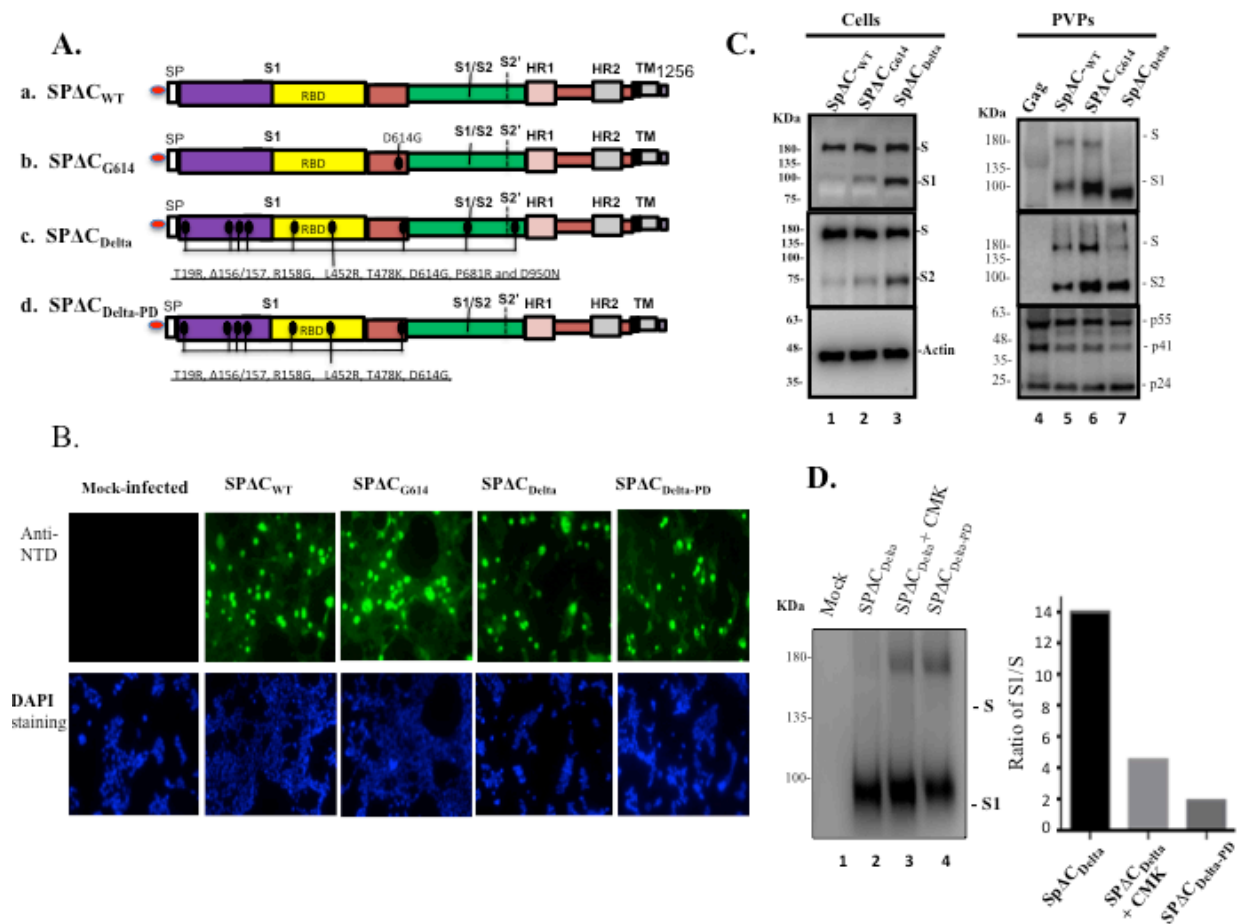
696 Zhu, H., Chen, C.Z., Sakamuru, S., Zhao, J., Ngan, D.K., Simeonov, A., Hall, M.D., Xia, M., Zheng, W., and  
697 Huang, R. (2021). Mining of high throughput screening database reveals AP-1 and autophagy pathways  
698 as potential targets for COVID-19 therapeutics. *Scientific Reports* *11*, 6725.

699 Zhu, N., D. Zhang, W. Wang, X. Li, B. Yang, J. Song, X. Zhao, B. Huang, W. Shi, and R. Lu. , and al., e.  
700 (2020). A novel coronavirus from patients with pneumonia in China, 2019. *New England Journal of*  
701 *Medicine* *382*, 727-733.

702

703

704



705

706

707 **Figure 1. The expression and cleavage of SARS-CoV-2 Delta Spike protein (SP) in the cells**

708 **and in the pseudotyped virus particles (PVPs).** (A) Schematic representation of the structure

709 domains and mutations of SARS-CoV-2 SP and its variants. A C-terminal 17aa of each of

710 SARS-CoV-2 SPAC was deleted in order to increase the incorporation of SP into the virrus

711 particles. (B) 293T cells were transfected with pCAGGS-SPAC<sub>wt</sub>, -SPAC<sub>G614</sub>, -SPAC<sub>Delta</sub> or -

712 SPAC<sub>Delta-PD</sub>. The intracellular expression of each SPAC in the transfected 293T cells were

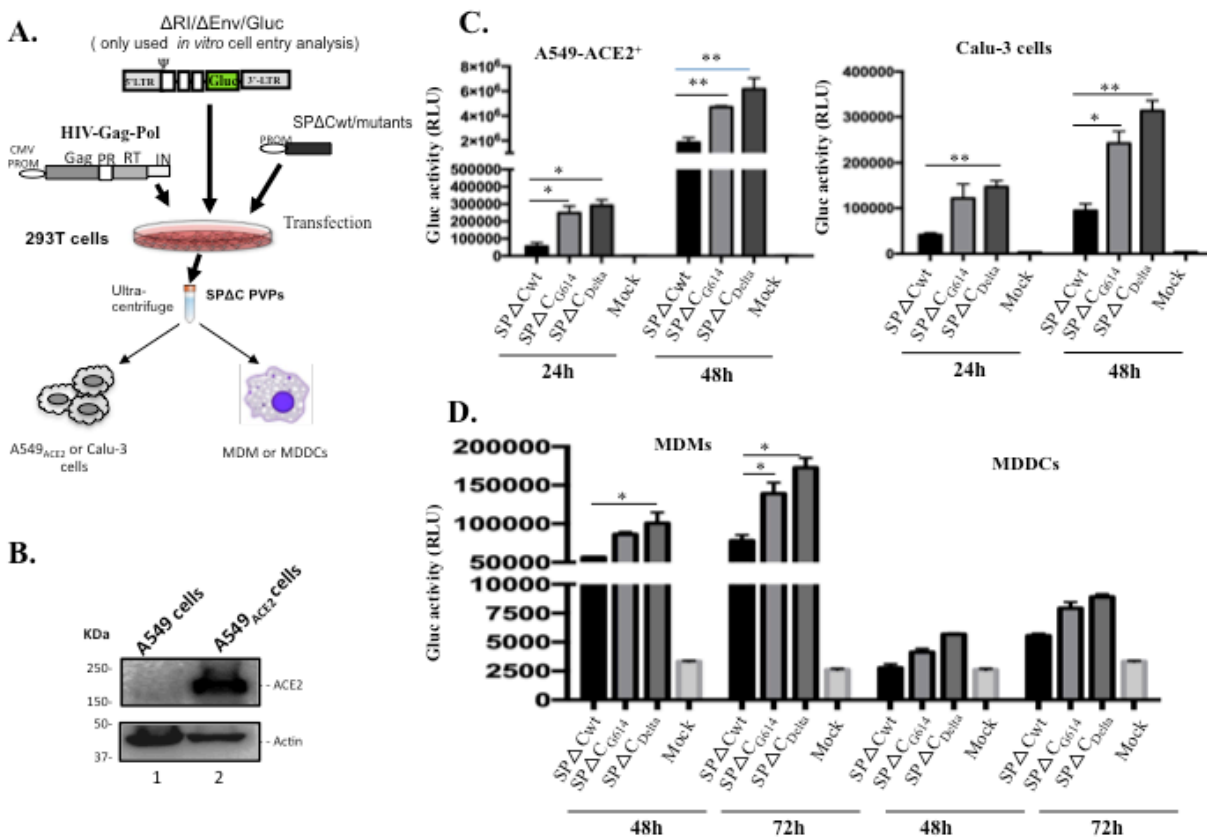
713 detected by immunofluorescence assay with SARS-CoV-2 S-NTD antibody. (C) 293T cells were

714 transfected with each SPAC-expressing plasmid, HIV ΔRI/Env<sup>-</sup>/Gluc) and a packaging plasmid

715 (pCMVΔ8.2) in HEK293T cells. As Gag-control, 293T cells were only transfected with

716 pCMV $\Delta$ 8.2 plasmid. WB were used to detect the expression and cleavage of various SP $\Delta$ C and  
 717 HIV Gag protein in cells and in PVPs. Full-length spike (S), cleaved S1 and S2 were annotated.  
 718 (D) SP $\Delta$ C<sub>Delta</sub>-PVPs were produced in the absence or in the presence of a furin inhibitor (CMK)  
 719 (25 $\mu$ M) and SP $\Delta$ C<sub>Delta</sub>PD-PVPs were analyzed by WB using polyclonal anti-SP/RBD antibody  
 720 (Left panel). The ratio of S1 relative to the full length SP was also quantified by laser  
 721 densitometry as indication of SP processing efficiencies (Right panel). Panel C-D show the  
 722 representative WB image from three independent experiments.

723

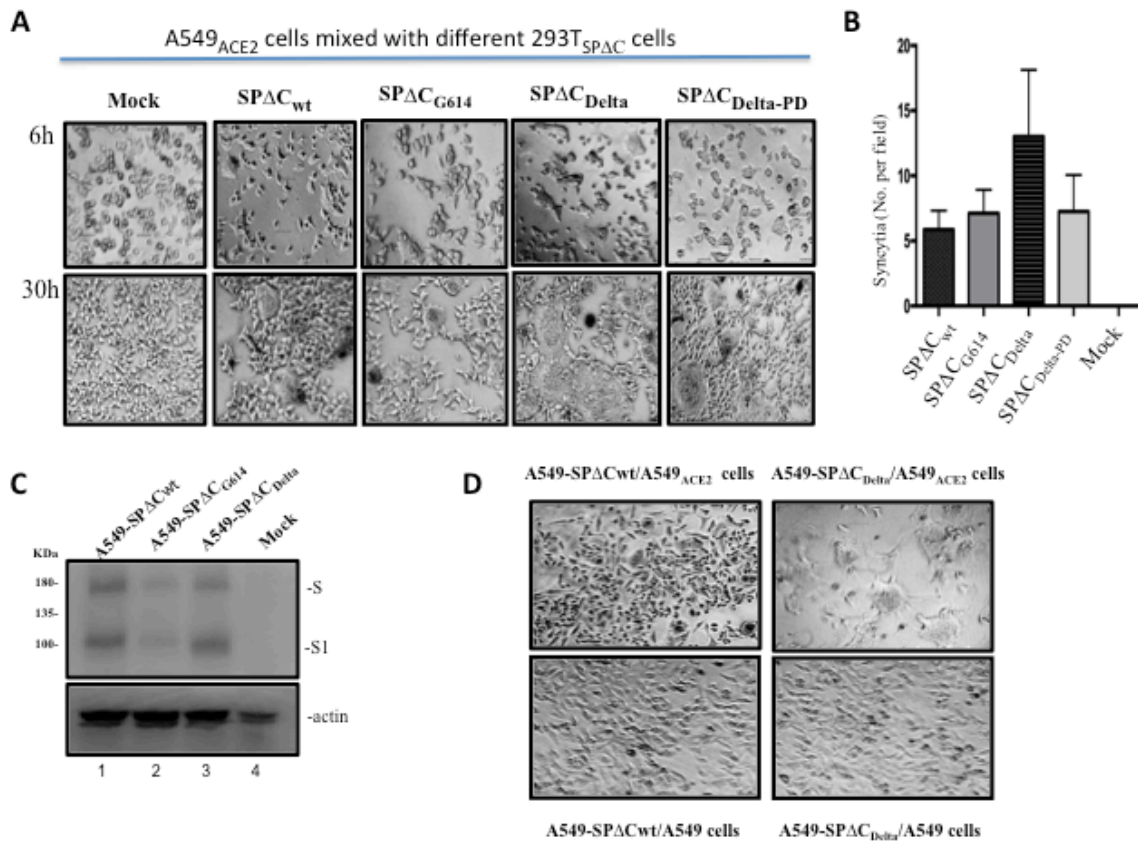


724

725 **Figure 2. SP pseudotyped virus infectivity assays on human lung cell lines, human**  
 726 **macrophages (MDMs) and dendritic cells (MDDCs).** (A) Schematic representation of the

727 procedures and the plasmids used for production of SARS-COV2-SP $\Delta$ C-pseudotyped  
728 lentivirus particles (SP $\Delta$ C-PVPs). (B) an A549<sub>ACE2</sub> cell line was generated by transducing  
729 A549 cells with a lentiviral vector ( pLenti-C-ACE2). The ACE2 expression in the transduced  
730 cells was detected by WB using anti-ACE2 antibody. (C, D) A549<sub>ACE2</sub>, Calu-3 cell lines,  
731 human MDMs or MDDCs were infected with an equal amount of SP $\Delta$ C<sub>wt</sub>, -SP $\Delta$ C<sub>G614</sub>, or -  
732 SP $\Delta$ C<sub>Delta</sub>-PVPs carrying Gaussia luciferase (Gluc) gene (adjusted by P24). At different time  
733 points, the Gluc activity in the supernatant of infected cultures was measured. The results are  
734 the mean values  $\pm$  standard deviations (SD) of two independent experiments. Statistically  
735 significant differences (\*  $P \leq 0.05$ ; \*\*,  $P \leq 0.01$ ) versus the SP $\Delta$ C<sub>wt</sub> were determined by  
736 unpaired t test. No significant (ns) was not shown.

737



738

739 **Figure 3. Delta-SP variant enhanced syncytia formation in lung epithelia cell line. (A)**

740 A549<sub>ACE2</sub> cells were cocultured with 293T cells transfected with SPΔC or variants. The syncytia

741 formation was monitored by microscopy at 6 hours and 30 hours after coculture. (B)

742 Quantification of the numbers of syncytia formation in the cocultures at 6 hrs under bright-field

743 microscopy. Results are the mean values ± standard deviations (SD) from two independent

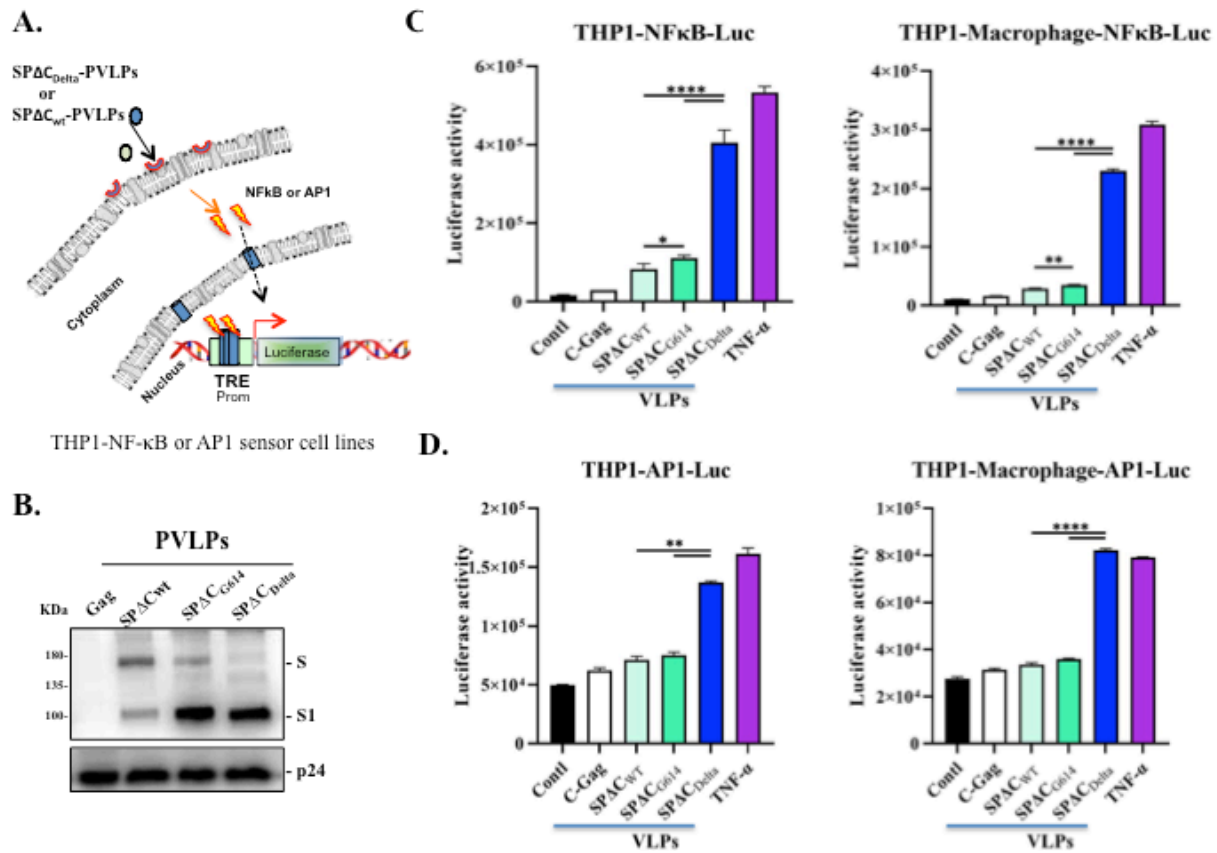
744 experiments. C) Expression of SPΔC<sub>wt</sub>, SPΔC<sub>G614</sub>, or SPΔC<sub>Delta</sub> in corresponding A549 stably

745 cell lines was detected by WB using anti-SP/RBD antibody. D) A549<sub>ACE2</sub> cells or A549 cells

746 were cocultured with A549-SPΔC<sub>wt</sub> or A549-SPΔC<sub>Delta</sub> stable cells. The syncytia formation was

747 visualized by microscopy at 30 hours after co-culture.

748



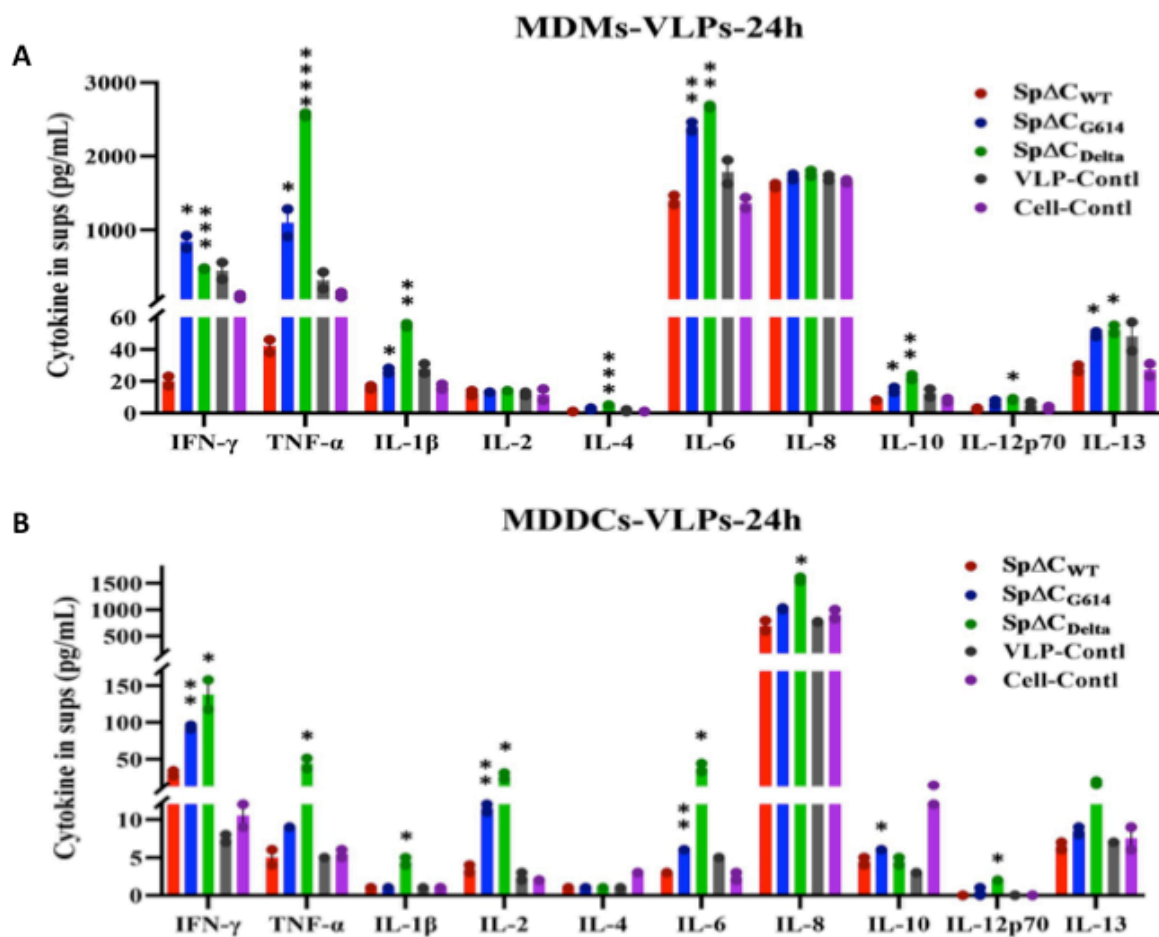
749

750 **Figure 4. SPAC<sub>Delta</sub>-PVLVPs stimulated NF-κB and Ap1-signal pathway in THP1 cells and**  
 751 **THP1 derived macrophages.** (A) The schematic diagram of NF-κB activity luciferase  
 752 reporter assay. The THP1-NF-κB -Luc, or THP1-AP1-Luc sensor cell line were incubated with  
 753 SPAC<sub>wt</sub>, -SPAC<sub>G614</sub>, or -SPAC<sub>Delta</sub>-PVLVPs for 6 hrs, and the activation of NF-κB or AP1  
 754 signaling was detected by measurement of the luciferase activity. (B) WB detected the  
 755 incorporation of SPAC<sub>wt</sub>, -SPAC<sub>G614</sub>, or -SPAC<sub>Delta</sub> in PVLVPs using SARS-CoV-2 S-NTD  
 756 antibody. The GagP24 was detected using mouse anti-P24 antibody. (C, D) The THP1-NFκB-  
 757 Luc or THP1-NFκB-Luc-derived macrophages, and THP1-AP-1-Luc cells or THP1-AP-1-  
 758 Luc-derived macrophages were treated with equal amounts of SPAC<sub>wt</sub>, SPAC<sub>G614</sub> or SPAC<sub>Delta</sub>-  
 759 PVLVPs (adjusted by P24) for 6 hrs, and the activation of NF-κB or AP-1 signaling was



760 detected by measurement of the Luc activity. Meanwhile, Gag-VLPs or TNF- $\alpha$  treatment were  
 761 used as negative or positive control. The results are the mean values  $\pm$  standard deviations (SD)  
 762 of two independent experiments. Statistical significance was determined using unpaired t test,  
 763 and significant p values are represented with asterisks (\*P  $\leq$  0.05; \*\*P  $\leq$  0.01; \*\*\*P  $\leq$  0.001;  
 764 \*\*\*\* P  $\leq$  0.0001). No significant (ns) was not shown

765



766

767

768 **Figure 5. Sp $\Delta$ C<sub>Delta</sub>- PVLPS stimulated proinflammatory cytokines release in human**  
 769 **MDM and MDDCs.** Human MDMs (A) or MDDCs (B) were treated with equal amount of  
 770 SPAC<sub>wt</sub>, SPAC<sub>G614</sub> or SPAC<sub>Delta</sub>-PVLPS (adjusted by p24). Gag-VLPs treated and non-treated

771 MDMs or MDDCs were used as negative controls. After 24 hrs, the cell culture supernatants  
772 were collected and different cytokines, including IFN- $\gamma$ , IL-1 $\beta$ , IL-2, IL-4, IL-6, IL-8, IL-10,  
773 IL-12p70, IL-13, TNF- $\alpha$  were measured by MSD immunoassay (Meso Scale Discovery). The  
774 results are the mean values  $\pm$  standard deviations (SD) of two biologic replicates. Statistical  
775 significance was determined using unpaired t test, and significant p values are represented with  
776 asterisks (\*P  $\leq$ 0.05; \*\*P  $\leq$  0.01; \*\*\*P $\leq$ 0.001; \*\*\*\* P $\leq$ 0.0001). No significant (ns) was not  
777 shown.

778